EARTHQUAKE ENGINEERING AND STRUCTURAL DYNAMICS, VOL. 26, 797–813 (1997)

DYNAMICS OF SEISMIC IMPACTS IN BASE-ISOLATED BUILDINGS

PRAVEEN K. MALHOTRA*
Adjunct Faculty, California State University, Sacramento, CA 95819-6029, U.S.A.

SUMMARY

A systematic study is made of the effects of seismic impacts between the base of an isolated building and the surrounding retaining wall. The analysis is performed without using gap elements or assuming values of the coefficient of restitution and the duration of impact. The analysis captures the effects of wave travel along the height of the building and of the associated energy loss. It poses no numerical difficulties. Results show that for elastic systems the base shear generated by impacts can be higher than the weight of the building; base shear increases with increase in the stiffness of the retaining wall, stiffness of the building and the mass of the base mat. A significant fraction of the initial kinetic energy of the system is lost by impacts; energy loss increases with increase in the stiffness of the retaining wall, system damping and mass of the base mat. © 1997 by John Wiley & Sons, Ltd.

Earthquake Engng. Struct. Dyn., **26**, 797–813 (1997)

No. of Figures: 9. No. of Tables: 0. No. of References: 9.

KEY WORDS: base isolation; impact; building; seismic; separation gap

INTRODUCTION

In seismically isolated buildings, a separation gap is provided between the base of the building and the surrounding retaining wall to allow free movement of the base during strong ground shaking. During a less probable, stronger than expected, shaking it is possible that the width of the gap will not be sufficient and the base would impact the retaining wall or some other barrier device with a certain velocity.[1] Base impacts generate stress waves which travel along the height of the building and reflect from its top and bottom. Energy is lost as a result of wave travel and large forces are experienced by the building and the retaining wall.

Most previous studies of impacts in buildings and bridges have made use of gap elements, each comprising of a spring and a dashpot.[1–5] The spring controls the impact duration and the dashpot accounts for the loss of energy. Cross and Jones[6] determined the spring stiffness and the dashpot constant from assumed values of the impact duration and the coefficient of restitution. No rational guidelines are, however, available for selecting suitable values of the impact duration and the coefficient of restitution. Numerical results, naturally, depend upon the assumed values of these factors. Also, the use of very stiff spring poses numerical difficulties making the solution of impact with a rigid wall almost intractable.

A need is, therefore, felt for a numerically stable solution which captures the effects of impacts—forces generated and energy dissipated—without assuming the values of the impact duration, dashpot constant or the coefficient of restitution.

PROBLEM STATEMENT AND MODEL

A multi-storey base-isolated building, shown in Figure 1(a), is subjected to such a level of ground shaking that the base of the building impacts the surrounding retaining wall with a velocity v_0. It is desired to

* Correspondence to: Praveen K. Malhotra, 4941 Knightswood Way, Granite Bay, CA 95746, U.S.A. E-mail: pmalhotra@aol.com

CCC 0098–8847/97/080797–17$17·50

Received 30 August 1996
Revised 23 January 1997

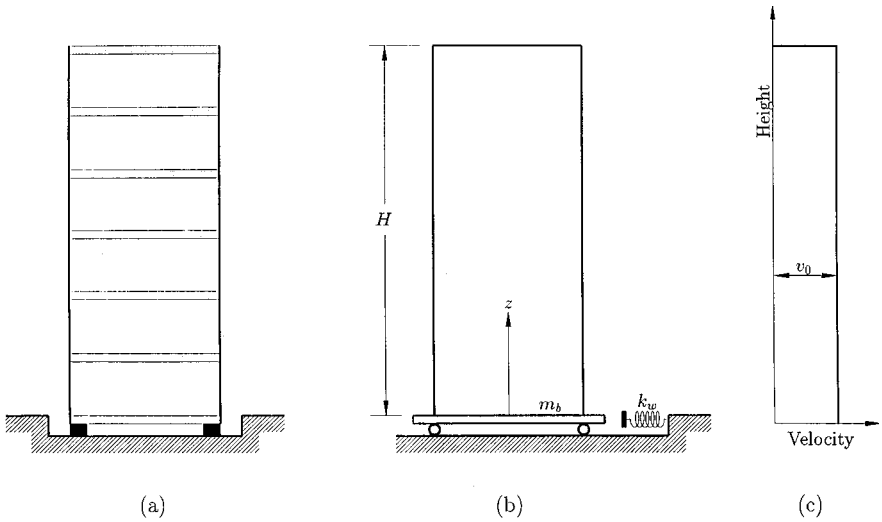

Figure 1. (a) Multi-storey base isolated building; (b) idealized model of building, isolator bearings and retaining wall; and (c) velocity distribution along the height of building at impact ($t = 0$)

determine (1) the base shear in the building, (2) the force in the retaining wall, and (3) the energy lost as a result of this impact.

The superstructure is modelled by a uniform shear beam of height H, cross-sectional area A, shear modulus G, and mass density ρ supported on a rigid base mat of mass m_b, as shown in Figure 1(b). The height of a point on the shear beam, measured from the top of the base mat, is denoted by z. The fundamental fixed-base period of the shear beam is

$$T_f = \frac{4H}{c} \tag{1}$$

where $c = \sqrt{G/\rho}$ is the shear wave velocity. The retaining wall is represented by a linear elastic spring of stiffness k_w. The building is assumed perfectly isolated; thus, before impact the entire building and the base mat move—as a rigid body—with the same initial velocity v_0, as shown in Figure 1(c). The effect of assuming perfect isolation is discussed later. The damping ratio for each vibration mode of the system, during and after impact, is assumed equal to ζ. The material non-linearity in the building and the retaining wall is not considered in this analysis.

METHOD OF ANALYSIS

The system responds in three stages: (1) before impact, it moves as a rigid body; (2) during impact, it responds in various modes of vibration of the building–retaining wall system; and (3) after separation, it responds in various modes of vibration of the building with no-shear boundary condition at the top of the building and below the base mass. No analysis is required for stage 1. Analysis for stages 2 and 3 is presented below.

During impact

At impact ($t = 0$), the velocity distribution along the height of the building is as shown in Figure 1(c). Using the first N natural modes of vibration of the building–retaining wall system, the velocity distribution may be expressed as

$$v(\xi, t = 0) = v_0 \approx \sum_{n=1}^{N} V_n \phi_n(\xi) \tag{2}$$

where $\xi = z/H$ is the normalized vertical co-ordinate and ϕ_n the nth mode shape, given by (Appendix II)

$$\phi_n(\xi) = \cos\left(\frac{\omega_n T_f}{4}\right)\cos\left(\frac{\omega_n T_f}{4}\xi\right) + \sin\left(\frac{\omega_n T_f}{4}\right)\sin\left(\frac{\omega_n T_f}{4}\xi\right) \tag{3}$$

The nth natural frequency ω_n (rad/s) is obtained from the solution of the characteristic equation

$$\tan\left(\frac{\omega_n T_f}{4}\right) = \left(\frac{T_f}{T_w}\right)^2\left(1 + \frac{m_b}{m}\right)\frac{\pi^2}{\omega_n T_f} - \frac{m_b}{m}\left(\frac{\omega_n T_f}{4}\right) \tag{4}$$

where

$$T_w = 2\pi\sqrt{\frac{m + m_b}{k_w}} \tag{5}$$

is the period of the system assuming the building to be rigid, and $m = \rho AH$ the mass of building excluding the base mat. The mass distribution (mass per unit ξ) for the system may be expressed as

$$\tilde{m}(\xi) = m + m_b\delta(\xi) \tag{6}$$

where δ is the Dirac delta function with the following properties:

$$\delta(\xi) = 0 \quad \text{for } \xi \neq 0 \tag{7a}$$

$$\int_0^1 \delta(\xi)\,\mathrm{d}\xi = 1 \tag{7b}$$

The V_n values in equation (2) are obtained by multiplying both sides of equation (2) with $\tilde{m}(\xi)\phi_n(\xi)$ and integrating along the height of the building, using the orthogonality condition,

$$\int_0^1 \tilde{m}(\xi)\phi_n(\xi)\phi_i(\xi)\,\mathrm{d}\xi = 0 \quad \text{for } \omega_n \neq \omega_i \tag{8}$$

This gives

$$V_n = v_0\frac{8\sin(\omega_n T_f/4) + 2\omega_n T_f(m_b/m)\cos(\omega_n T_f/4)}{\omega_n T_f + 2\sin(\omega_n T_f/2) + 2\omega_n T_f(m_b/m)\cos^2(\omega_n T_f/4)} \tag{9}$$

The displacement and velocity responses, obtained by summation of the free-vibration responses of the various modes (Reference 7, p. 391), are

$$u(\xi, t) = \sum_{n=1}^{N}\frac{V_n}{\omega_{nD}}\sin(\omega_{nD}t)\exp(-\zeta\omega_n t)\phi_n(\xi) \tag{10}$$

$$v(\xi, t) = \sum_{n=1}^{N} V_n\left\{\cos(\omega_{nD}t) - \frac{\zeta\omega_n}{\omega_{nD}}\sin(\omega_{nD}t)\right\}\exp(-\zeta\omega_n t)\phi_n(\xi) \tag{11}$$

where $\omega_{nD} = \omega_n\sqrt{1-\zeta^2}$ is the nth damped natural frequency of the system. The base displacement, obtained from equation (10), is

$$u_b(t) = u(0, t) = \sum_{n=1}^{N}\frac{V_n}{\omega_{nD}}\sin(\omega_{nD}t)\exp(-\zeta\omega_n t)\cos\left(\frac{\omega_n T_f}{4}\right) \tag{12}$$

and the base velocity, obtained from equation (11), is

$$v_b(t) = v(0, t) = \sum_{n=1}^{N} V_n\left\{\cos(\omega_{nD}t) - \frac{\zeta\omega_n}{\omega_{nD}}\sin(\omega_{nD}t)\right\}\exp(-\zeta\omega_n t)\cos\left(\frac{\omega_n T_f}{4}\right) \tag{13}$$

The momentum of the system is

$$M(t) = m\int_0^1 v(\xi, t)\,\mathrm{d}\xi + m_\mathrm{b} v_\mathrm{b}(t)$$
$$= m\sum_{n=1}^{N} V_n\left\{\cos(\omega_{n\mathrm{D}}t) - \frac{\zeta\omega_n}{\omega_{n\mathrm{D}}}\sin(\omega_{n\mathrm{D}}t)\right\}\exp(-\zeta\omega_n t)\frac{4}{\omega_n T_\mathrm{f}}\sin\left(\frac{\omega_n T_\mathrm{f}}{4}\right)$$
$$+ m_\mathrm{b}\sum_{n=1}^{N} V_n\left\{\cos(\omega_{n\mathrm{D}}t) - \frac{\zeta\omega_n}{\omega_{n\mathrm{D}}}\sin(\omega_{n\mathrm{D}}t)\right\}\exp(-\zeta\omega_n t)\cos\left(\frac{\omega_n T_\mathrm{f}}{4}\right) \tag{14}$$

The strain and kinetic energies of the system are

$$\mathrm{SE}(t) = \frac{GA}{2H}\int_0^1 \left\{\frac{\partial u(\xi, t)}{\partial\xi}\right\}^2 \mathrm{d}\xi + \frac{1}{2}k_\mathrm{w}u_\mathrm{b}^2(t) \tag{15}$$

$$\mathrm{KE}(t) = \frac{m}{2}\int_0^1 v^2(\xi, t)\,\mathrm{d}\xi + \frac{1}{2}m_\mathrm{b}v_\mathrm{b}^2(t) \tag{16}$$

Since the modes of vibration are orthogonal to each other, the strain and kinetic energies are obtained for each mode separately and then added to give the following expressions:

$$\mathrm{SE}(t) = \frac{m}{4(1-\zeta^2)}\sum_{n=1}^{N}\{V_n\sin(\omega_{n\mathrm{D}}t)\exp(-\zeta\omega_n t)\}^2\left\{1 - \frac{2}{\omega_n T_\mathrm{f}}\sin\left(\frac{\omega_n T_\mathrm{f}}{2}\right)\right\}$$
$$+ 2\pi^2 m_\mathrm{b}\left(\frac{T_\mathrm{f}}{T_\mathrm{w}}\right)^2\sum_{n=1}^{N}\left\{\frac{V_n}{\omega_{n\mathrm{D}}T_\mathrm{f}}\sin(\omega_{n\mathrm{D}}t)\exp(-\zeta\omega_n t)\cos\left(\frac{\omega_n T_\mathrm{f}}{4}\right)\right\}^2 \tag{17}$$

$$\mathrm{KE}(t) = \frac{m}{4}\sum_{n=1}^{N}\left[V_n\left\{\cos(\omega_{n\mathrm{D}}t) - \frac{\omega_n}{\omega_{n\mathrm{D}}}\sin(\omega_{n\mathrm{D}}t)\right\}\exp(-\zeta\omega_n t)\right]^2$$
$$\times\left\{1 + \frac{2}{\omega_n T_\mathrm{f}}\sin\left(\frac{\omega_n T_\mathrm{f}}{2}\right)\right\}$$
$$+ \frac{m_\mathrm{b}}{2}\sum_{n=1}^{N}\left[V_n\left\{\cos(\omega_{n\mathrm{D}}t) - \frac{\omega_n}{\omega_{n\mathrm{D}}}\sin(\omega_{n\mathrm{D}}t)\right\}\exp(-\zeta\omega_n t)\right]^2\cos^2\left(\frac{\omega_n T_\mathrm{f}}{4}\right) \tag{18}$$

The shear along the height of the building is

$$F_\mathrm{s}(\xi, t) = \frac{GA}{H}\frac{\partial u(\xi, t)}{\partial\xi}$$
$$= \frac{4m}{T_\mathrm{f}}\sum_{n=1}^{N}\frac{\omega_n V_n}{\omega_{n\mathrm{D}}}\cos(\omega_{n\mathrm{D}}t)\exp(-\zeta\omega_n t)$$
$$\times\left\{-\cos\left(\frac{\omega_n T_\mathrm{f}}{4}\right)\sin\left(\frac{\omega_n T_\mathrm{f}}{4}\xi\right) + \sin\left(\frac{\omega_n T_\mathrm{f}}{4}\right)\cos\left(\frac{\omega_n T_\mathrm{f}}{4}\xi\right)\right\} \tag{19}$$

and the base shear, obtained from equation (19), is

$$F_{\mathrm{sb}}(t) = F_\mathrm{s}(0, t) = \frac{4m}{T_\mathrm{f}}\sum_{n=1}^{N}\frac{\omega_n V_n}{\omega_{n\mathrm{D}}}\cos(\omega_{n\mathrm{D}}t)\exp(-\zeta\omega_n t)\sin\left(\frac{\omega_n T_\mathrm{f}}{4}\right) \tag{20}$$

The force in the retaining wall is

$$F_w(t) = k_w u_b(t) = k_w \sum_{n=1}^{N} \frac{V_n}{\omega_{nD}} \sin(\omega_{nD} t) \exp(-\zeta \omega_n t) \cos\left(\frac{\omega_n T_f}{4}\right) \tag{21}$$

After separation

The retaining wall and the base mat separate at $t = \tau$ when the force in the wall becomes zero, i.e. $F_w(\tau) = 0$. At separation, the displacement and velocity along the height of the building are obtained by substituting $t = \tau$ in equations (10) and (11), respectively. These are

$$u(\xi, \tau) = \sum_{n=1}^{N} \frac{V_n}{\omega_{nD}} \sin(\omega_{nD} \tau) \exp(-\zeta \omega_n \tau) \phi_n(\xi) \tag{22}$$

$$v(\xi, \tau) = \sum_{n=1}^{N} V_n \left\{ \cos(\omega_{nD} \tau) - \frac{\zeta \omega_n}{\omega_{nD}} \sin(\omega_{nD} \tau) \right\} \exp(-\zeta \omega_n \tau) \phi_n(\xi) \tag{23}$$

The displacement and velocity at $t = \tau$ may also be expressed in terms of the first $\bar{N}$ modes of vibration of the system after separation, i.e.

$$u(\xi, \tau) \approx \sum_{\bar{n}=1}^{\bar{N}} U_{\bar{n}} \phi_{\bar{n}}(\xi) \tag{24}$$

$$v(\xi, \tau) \approx \sum_{\bar{n}=1}^{\bar{N}} V_{\bar{n}} \phi_{\bar{n}}(\xi) \tag{25}$$

where the mode shapes after separation are given by

$$\phi_{\bar{n}}(\xi) = \cos\left(\frac{\omega_{\bar{n}} T_f}{4}\right) \cos\left(\frac{\omega_{\bar{n}} T_f}{4} \xi\right) + \sin\left(\frac{\omega_{\bar{n}} T_f}{4}\right) \sin\left(\frac{\omega_{\bar{n}} T_f}{4} \xi\right) \tag{26}$$

and the $\bar{n}$th natural frequency $\omega_{\bar{n}}$ is obtained from the solution of the characteristic equation

$$\tan\left(\frac{\omega_{\bar{n}} T_f}{4}\right) = -\frac{m_b}{m}\left(\frac{\omega_{\bar{n}} T_f}{4}\right) \tag{27}$$

Equation (27) is obtained by substituting $k_w = 0$ (or $T_w = \infty$) in equation (4). The first mode, obtained from equations (26) and (27), is a rigid-body mode with $\phi_{\bar{n}} = 1$ and $\omega_{\bar{n}} = 0$.

The $U_{\bar{n}}$ and $V_{\bar{n}}$ values in equations (24) and (25) are obtained by equating equation (22) with equation (24), and equation (23) with equation (25), multiplying both sides with $\tilde{m}(\xi)\phi_{\bar{n}}(\xi)$, and integrating along the height of the building (using the orthogonality property of the modes of vibration). This gives

$$\begin{aligned} U_{\bar{n}} = \Bigg[& 2 \sum_{n=1}^{N} \left\{ U_n \cos(\omega_{nD} \tau) + \frac{\zeta \omega_n U_n + V_n}{\omega_{nD}} \sin(\omega_{nD} \tau) \right\} \exp(-\zeta \omega_n \tau) \\ & \times \left\{ \frac{\sin((\omega_n T_f + \omega_{\bar{n}} T_f)/4)}{\omega_n T_f + \omega_{\bar{n}} T_f} + \frac{\sin((\omega_n T_f - \omega_{\bar{n}} T_f)/4)}{\omega_n T_f - \omega_{\bar{n}} T_f} \right\} \\ & + \frac{m_b}{m} \sum_{n=1}^{N} \left\{ U_n \cos(\omega_{nD} \tau) + \frac{\zeta \omega_n U_n + V_n}{\omega_{nD}} \sin(\omega_{nD} \tau) \right\} \exp(-\zeta \omega_n \tau) \\ & \times \cos\left(\frac{\omega_n T_f}{4}\right) \cos\left(\frac{\omega_{\bar{n}} T_f}{4}\right) \Bigg] \div \left[\frac{1}{2} + \frac{\sin(\omega_{\bar{n}} T_f/2)}{\omega_{\bar{n}} T_f} + \frac{m_b}{m} \cos^2\left(\frac{\omega_{\bar{n}} T_f}{4}\right) \right] \end{aligned} \tag{28}$$

$$V_{\bar{n}} = \left[2 \sum_{n=1}^{N} \left\{ V_n \cos(\omega_{n\mathrm{D}}\tau) - \frac{\omega_n U_n + \zeta V_n}{\sqrt{1-\zeta^2}} \sin(\omega_{n\mathrm{D}}\tau) \right\} \exp(-\zeta\omega_n\tau) \right.$$
$$\times \left\{ \frac{\sin((\omega_n T_\mathrm{f} + \omega_{\bar{n}} T_\mathrm{f})/4)}{\omega_n T_\mathrm{f} + \omega_{\bar{n}} T_\mathrm{f}} + \frac{\sin((\omega_n T_\mathrm{f} - \omega_{\bar{n}} T_\mathrm{f})/4)}{\omega_n T_\mathrm{f} - \omega_{\bar{n}} T_\mathrm{f}} \right\}$$
$$+ \frac{m_\mathrm{b}}{m} \sum_{n=1}^{N} \left\{ V_n \cos(\omega_{n\mathrm{D}}\tau) - \frac{\omega_n U_n + \zeta V_n}{\sqrt{1-\zeta^2}} \sin(\omega_{n\mathrm{D}}\tau) \right\} \exp(-\zeta\omega_n\tau)$$
$$\left. \times \cos\left(\frac{\omega_n T_\mathrm{f}}{4}\right) \cos\left(\frac{\omega_{\bar{n}} T_\mathrm{f}}{4}\right) \right] \div \left[\frac{1}{2} + \frac{\sin(\omega_{\bar{n}} T_\mathrm{f}/2)}{\omega_{\bar{n}} T_\mathrm{f}} + \frac{m_\mathrm{b}}{m} \cos^2\left(\frac{\omega_{\bar{n}} T_\mathrm{f}}{4}\right) \right] \tag{29}$$

The displacement and velocity responses are then obtained as

$$u(\xi, \bar{t}) = \sum_{\bar{n}=1}^{\bar{N}} \left\{ U_{\bar{n}} \cos(\omega_{\bar{n}\mathrm{D}}\bar{t}) + \frac{\zeta\omega_{\bar{n}} U_{\bar{n}} + V_{\bar{n}}}{\omega_{\bar{n}\mathrm{D}}} \sin(\omega_{\bar{n}\mathrm{D}}\bar{t}) \right\} \exp(-\zeta\omega_{\bar{n}}\bar{t}) \phi_{\bar{n}}(\xi) \tag{30}$$

$$v(\xi, \bar{t}) = \sum_{\bar{n}=1}^{\bar{N}} \left\{ V_{\bar{n}} \cos(\omega_{\bar{n}\mathrm{D}}\bar{t}) - \frac{\omega_{\bar{n}} U_{\bar{n}} + \zeta V_{\bar{n}}}{\sqrt{1-\zeta^2}} \sin(\omega_{\bar{n}\mathrm{D}}\bar{t}) \right\} \exp(-\zeta\omega_{\bar{n}}\bar{t}) \phi_{\bar{n}}(\xi) \tag{31}$$

where $\bar{t} = t - \tau$ is the time after separation. The displacement and velocity of the base are

$$u_\mathrm{b}(\bar{t}) = \sum_{\bar{n}=1}^{\bar{N}} \left\{ U_{\bar{n}} \cos(\omega_{\bar{n}\mathrm{D}}\bar{t}) + \frac{\zeta\omega_{\bar{n}} U_{\bar{n}} + V_{\bar{n}}}{\omega_{\bar{n}\mathrm{D}}} \sin(\omega_{\bar{n}\mathrm{D}}\bar{t}) \right\} \exp(-\zeta\omega_{\bar{n}}\bar{t}) \cos\left(\frac{\omega_{\bar{n}} T_\mathrm{f}}{4}\right) \tag{32}$$

$$v_\mathrm{b}(\bar{t}) = \sum_{\bar{n}=1}^{\bar{N}} \left\{ V_{\bar{n}} \cos(\omega_{\bar{n}\mathrm{D}}\bar{t}) - \frac{\omega_{\bar{n}} U_{\bar{n}} + \zeta V_{\bar{n}}}{\sqrt{1-\zeta^2}} \sin(\omega_{\bar{n}\mathrm{D}}\bar{t}) \right\} \exp(-\zeta\omega_{\bar{n}}\bar{t}) \cos\left(\frac{\omega_{\bar{n}} T_\mathrm{f}}{4}\right) \tag{33}$$

The momentum of the system is

$$M(\bar{t}) = m \sum_{\bar{n}=1}^{\bar{N}} \left\{ V_{\bar{n}} \cos(\omega_{\bar{n}\mathrm{D}}\bar{t}) - \frac{\omega_{\bar{n}} U_{\bar{n}} + \zeta V_{\bar{n}}}{\sqrt{1-\zeta^2}} \sin(\omega_{\bar{n}\mathrm{D}}\bar{t}) \right\} \exp(-\zeta\omega_{\bar{n}}\bar{t})$$
$$\times \frac{4}{\omega_{\bar{n}} T_\mathrm{f}} \sin\left(\frac{\omega_{\bar{n}} T_\mathrm{f}}{4}\right) + m_\mathrm{b} \sum_{\bar{n}=1}^{\bar{N}} \left\{ V_{\bar{n}} \cos(\omega_{\bar{n}\mathrm{D}}\bar{t}) - \frac{\omega_{\bar{n}} U_{\bar{n}} + \zeta V_{\bar{n}}}{\sqrt{1-\zeta^2}} \sin(\omega_{\bar{n}\mathrm{D}}\bar{t}) \right\}$$
$$\times \exp(-\zeta\omega_{\bar{n}}\bar{t}) \cos\left(\frac{\omega_{\bar{n}} T_\mathrm{f}}{4}\right) \tag{34}$$

The strain and kinetic energies are

$$\mathrm{SE}(\bar{t}) = \frac{m}{2} \sum_{\bar{n}=1}^{\bar{N}} \left[\left\{ \omega_{\bar{n}} U_{\bar{n}} \cos(\omega_{\bar{n}\mathrm{D}}\bar{t}) + \frac{\zeta\omega_{\bar{n}} U_{\bar{n}} + V_{\bar{n}}}{\sqrt{1-\zeta^2}} \sin(\omega_{\bar{n}\mathrm{D}}\bar{t}) \right\} \exp(-\zeta\omega_{\bar{n}}\bar{t}) \right]^2$$
$$\times \left\{ \frac{1}{2} - \frac{\sin(\omega_{\bar{n}} T_\mathrm{f}/2)}{\omega_{\bar{n}} T_\mathrm{f}} \right\} \tag{35}$$

$$\mathrm{KE}(\bar{t}) = \frac{m}{2}\sum_{\bar{n}=1}^{\bar{N}}\left[\left\{V_{\bar{n}}\cos(\omega_{\bar{n}\mathrm{D}}\bar{t}) + \frac{\omega_{\bar{n}}U_{\bar{n}} + \zeta V_{\bar{n}}}{\sqrt{1-\zeta^2}}\sin(\omega_{\bar{n}\mathrm{D}}\bar{t})\right\}\exp(-\zeta\omega_{\bar{n}}\bar{t})\right]^2$$
$$\times\left\{\frac{1}{2} + \frac{\sin(\omega_{\bar{n}}T_\mathrm{f}/2)}{\omega_{\bar{n}}T_\mathrm{f}}\right\}$$
$$+\frac{m_\mathrm{b}}{2}\sum_{\bar{n}=1}^{\bar{N}}\left[\left\{\frac{\omega_{\bar{n}}U_{\bar{n}} + \zeta V_{\bar{n}}}{\sqrt{1-\zeta^2}}\sin(\omega_{\bar{n}\mathrm{D}}\bar{t}) - V_{\bar{n}}\cos(\omega_{\bar{n}\mathrm{D}}\bar{t})\right\}\exp(-\zeta\omega_{\bar{n}}\bar{t})\right]^2$$
$$\times\cos^2\left(\frac{\omega_{\bar{n}}T_\mathrm{f}}{4}\right) \tag{36}$$

Note that both SE and KE decay with time. Whereas, SE becomes zero in infinite time, KE approaches a value of $(m + m_\mathrm{b})V_1^2/2$—kinetic energy of the first (rigid-body) mode after separation.

The base shear is

$$F_\mathrm{sb}(\bar{t}) = \frac{GA}{H}\frac{\partial u}{\partial\xi}\bigg|_{\xi=0} = 4\frac{m}{T_\mathrm{f}}\sum_{\bar{n}=1}^{\bar{N}}\left\{\omega_{\bar{n}}U_{\bar{n}}\cos(\omega_{\bar{n}\mathrm{D}}\bar{t}) + \frac{\zeta\omega_{\bar{n}}U_{\bar{n}} + V_{\bar{n}}}{\sqrt{1-\zeta^2}}\sin(\omega_{\bar{n}\mathrm{D}}\bar{t})\right\}$$
$$\times\exp(-\zeta\omega_{\bar{n}}\bar{t})\sin\left(\frac{\omega_{\bar{n}}T_\mathrm{f}}{4}\right) \tag{37}$$

and the force in the retaining wall is

$$F_\mathrm{w}(\bar{t}) = k_\mathrm{w}u_\mathrm{b}(\bar{t}) = k_\mathrm{w}\sum_{\bar{n}=1}^{\bar{N}}\left\{U_{\bar{n}}\cos(\omega_{\bar{n}\mathrm{D}}\bar{t}) + \frac{\zeta\omega_{\bar{n}}U_{\bar{n}} + V_{\bar{n}}}{\omega_{\bar{n}\mathrm{D}}}\sin(\omega_{\bar{n}\mathrm{D}}\bar{t})\right\}$$
$$\times\exp(-\zeta\omega_{\bar{n}}\bar{t})\cos\left(\frac{\omega_{\bar{n}}T_\mathrm{f}}{4}\right) \tag{38}$$

NUMERICAL RESULTS

Solution without base mass

Shown in Figure 2(a) are the results of timewise variation of the base shear F_sb for different values of $T_\mathrm{w}/T_\mathrm{f}$. Lower the value of $T_\mathrm{w}/T_\mathrm{f}$, stiffer the retaining wall; $T_\mathrm{w}/T_\mathrm{f} = 0$ implies an infinitely stiff retaining wall. Results shown are for damping ratio $\zeta = 0{\cdot}04$ and base mass $m_\mathrm{b} = 0$ (the force in the retaining wall is, therefore, same as the base shear). Solutions were obtained using $N = \bar{N} = 250$. (A large number of modes are excited by impacts.) Results remained practically unchanged when the number of modes was increased to 500. The base shear in these plots is normalized with respect to mv_0/T_f and the time t is normalized with respect to T_f. Note that the stress pulse for $T_\mathrm{w}/T_\mathrm{f} = 0$ (rigid wall) is nearly rectangular, with a maximum value slightly less than $4mv_0/T_\mathrm{f}$, and duration $T_\mathrm{f}/2$. A simple solution using one-dimensional wave propagation analysis[8] would show that, for an undamped case, the stress pulse would be rectangular, of magnitude $4mv_0/T_\mathrm{f}$, and duration $T_\mathrm{f}/2$. Presence of damping slightly reduced the magnitude of the stress pulse, changed its shape, but did not affect its duration.

If a building with no base mass and a fixed-base period $T_\mathrm{f} = 0{\cdot}2$ s were to impact a rigid retaining wall with a velocity $v_0 = 50$ cm/s, the maximum base shear $(F_\mathrm{sb})_\mathrm{max}$ would be $4 \times m \times 50/0{\cdot}2 \approx mg$ = the weight of the building, and the duration of impact τ would be $0{\cdot}2/2 = 0{\cdot}1$ s. With increase in wall flexibility, the base shear would reduce, the shape of the force pulse change gradually from rectangular to half-sine, and the duration of impact increase, as seen in Figure 2(a).

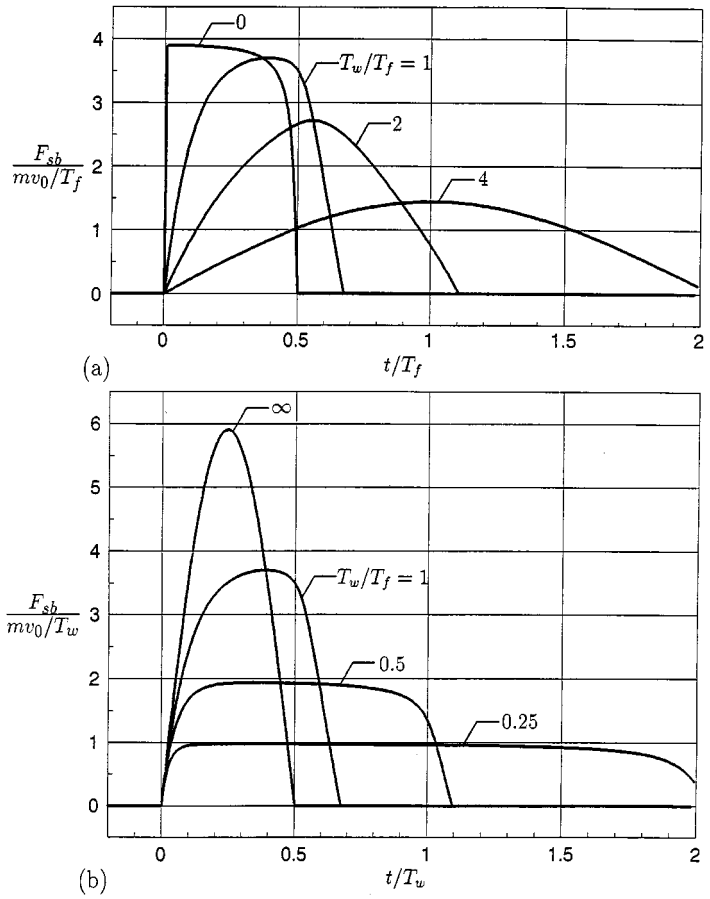

Figure 2. Timewise variation of base shear generated by impact, for different values of retaining wall stiffness. Results are normalized with respect to (a) building stiffness, and (b) retaining wall stiffness ($\zeta = 0{\cdot}04$, $m_b/m = 0$)

Since the base shear F_{sb} and the time t in Figure 2(a) are both normalized with respect to T_f, the effect of varying the building stiffness (or T_f) is not clear in this figure. This effect is more clear in Figure 2(b) in which the base shear and time t are normalized with respect to T_w (or wall stiffness). The value of $T_w/T_f = \infty$ implies a rigid building. The analysis of a single-degree-freedom system (of mass m, period T_w, damping ζ, and initial velocity v_0) would show that the force pulse for the rigid building is half-sine, with a maximum value $\approx 2\pi \exp(-\zeta\pi/2) mv_0/T_w \approx 5{\cdot}9mv_0/T_w$ (for $\zeta = 0{\cdot}04$) and duration $T_w/2$ (Reference 7, p. 45). As the building becomes flexible, the magnitude of the pulse reduces, and its shape changes gradually from half-sine to rectangular, as seen in Figure 2(b). The shape of the stress pulse, therefore, depends on the ratio T_w/T_f, while the magnitude of the pulse depends on the actual values of T_w and T_f.

Travelling wave effect

For a rigid retaining wall ($T_w/T_f = 0$), the shear distribution along the height of the building, at different times after the impact, is shown in Figure 3. Note that the wave front travels a distance of $0{\cdot}4H$ in time $0{\cdot}1T_f$ as would be expected from equation (1). The wave reflects from the top of the building (free end) as a negative shear wave at $t = 0{\cdot}25T_f$; it reaches the base and cancels the positive shear wave at $t = 0{\cdot}5T_f$, resulting in a loss of contact. Similar wave travel effect was observed in the strong-motion records recovered from

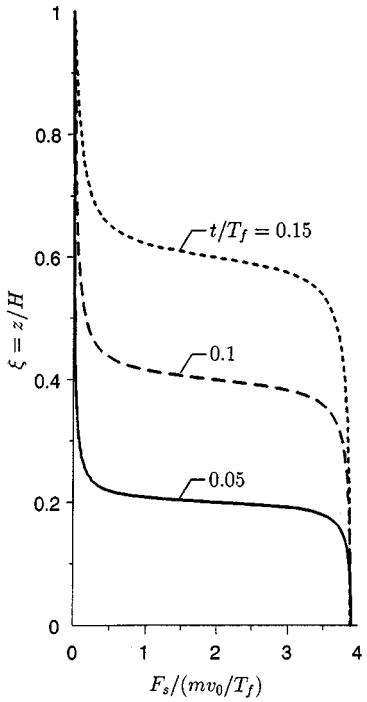

Figure 3. Distribution of shear force along the height of building at different times after an impact at the base ($\zeta = 0{\cdot}04$, $m_b/m = 0$)

a seismically instrumented concrete bridge which experienced significant pounding at its expansion joints during the 1992 Landers and Big Bear earthquakes in Southern California.[9]

Effect of base mass

In the presence of a base mass, the force in the retaining wall F_w is no longer equal to the base shear F_{sb}. Plots of F_{sb} and F_w, for $m_b/m = 0{\cdot}2$ and two different values of T_w/T_f, are shown in Figures 4(a) and 4(b), respectively. Note that for the stiffer wall, the forces (F_{sb} and F_w) with the base mass considered are significantly higher than those without the base mass [Figure 2(a)]. Both F_{sb} and F_w oscillate about a value of $4mv_0/T_f$ with a period equal to the period of base mass–retaining wall system ($2\pi\sqrt{m_b/k_w}$). The amplitude of oscillations is so large that at time $t = 0{\cdot}072T_f$ the force in the retaining wall becomes zero and a momentary loss of contact occurs between the base mass and the retaining wall. The contact is quickly re-established at $t = 0{\cdot}091T_f$ because the momentum of the overall system is still positive—the system still has a tendency to move to the right—as seen in Figure 5(a). Note that the momentum stays constant during momentary separation ($0{\cdot}072T_f < t < 0{\cdot}091T_f$) and final separation ($t > 0{\cdot}526T_f$). The momentum changes from $(m + m_b)v_0$ to $-0{\cdot}723\,(m + m_b)v_0$ in time $0{\cdot}526T_f$. The net change of $1{\cdot}723\,(m + m_b)\,v_0$ equals the area under the force pulse $F_w(t)$ in Figure 4(b); the average rate of change of $3{\cdot}276\,(m + m_b)v_0/T_f = 3{\cdot}931mv_0/T_f$ (for $m_b/m = 0{\cdot}2$) is the average value of F_w during impact. The presence of the base mass, therefore, did not affect the average value of the impact force but increased its maximum value significantly.

Energy loss

Before an impact, the only energy present is the kinetic energy due to rigid-body motion of the building. During impact a part of this energy is transferred to the higher internal modes of vibration and is lost when these modes finally damp out. The plots of timewise variation of the kinetic, strain and total energy of the

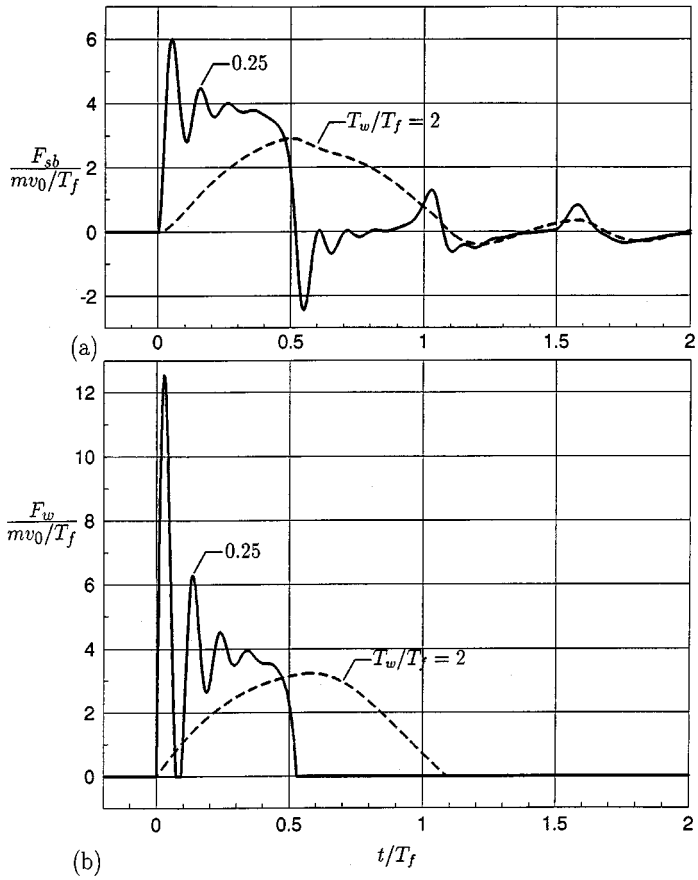

Figure 4. Timewise variation of (a) base shear; and (b) force in the retaining wall, for nonzero value of the base mass and two different values of the retaining wall stiffness ($\zeta = 0{\cdot}04$, $m_b/m = 0{\cdot}2$)

system are shown in Figure 5(b). For these plots, $m_b/m = 0{\cdot}2$, $T_w/T_f = 0{\cdot}25$, and the damping ratio $\zeta = 0{\cdot}04$. The system loses 39 per cent of its energy during impact ($0 < t < 0{\cdot}526T_f$), 43 per cent till $t = T_f$ and 48 per cent in infinite time (as seen later). Majority of the energy loss, therefore, occurs during the first fixed-base period of the system.

Plots of timewise variation of the total energy of the system for different values of T_w/T_f are shown in Figure 6(a). Note that the energy loss increases with increase in the stiffness of the retaining wall. For a very flexible retaining wall, the higher modes are not sufficiently excited, as a result, the building continues to move as a rigid body, during and after the impact, hence the loss of energy is small. As expected, an increase in system damping also increases the energy loss [Figure 6(b)].

The net energy lost by impact E_ℓ is computed by subtracting the kinetic energy of the rigid-body motion after separation from the kinetic energy of the system before impact, i.e.

$$E_\ell = \tfrac{1}{2}(m + m_b)v_0^2 - \tfrac{1}{2}(m + m_b)V_1^2 \tag{39}$$

The net energy loss E_ℓ is therefore determined without continuing the analysis after separation. Figure 7 shows the effects of ζ, T_w/T_f, and mass ratio m_b/m on energy loss E_ℓ. With increase in the wall stiffness, the net energy loss increases. An increase in damping ratio also increases the energy loss. Note that even for an undamped system ($\zeta = 0$), energy loss $E_\ell \neq 0$ for all values of T_w/T_f. For undamped case, E_ℓ is simply the

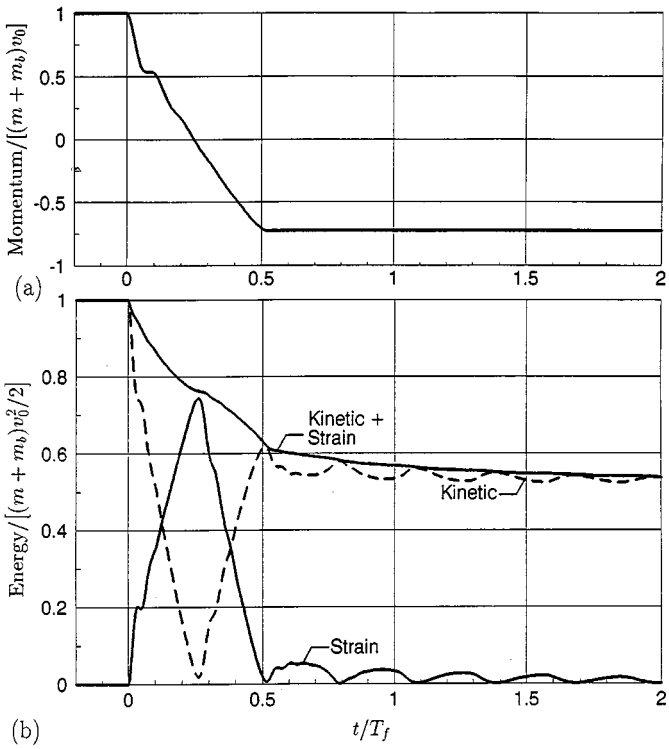

Figure 5. Timewise variation of (a) momentum of the system; and (b) kinetic, strain and total energies of the system ($\zeta = 0{\cdot}04$, $m_b/m = 0{\cdot}2$, $T_w/T_f = 0{\cdot}25$)

energy transferred to the higher internal modes of vibration. Even for a lightly damped system this energy is eventually lost; only for an idealized undamped system this energy is preserved in the higher internal modes of vibration.

An increase in the base mass increases the energy loss, because the presence of base mass increases the higher mode response.

Energy loss by radiation

When the base of the building impacts the retaining wall, stress waves are generated in the surrounding soil similar to those in the building. Radiation of these waves away from the building provides an additional sources of energy loss. Relative importance of radiation energy loss increases with increase in the flexibility of the retaining wall compared to that of the building. Although, no rational guidelines are available to consider the radiation energy loss for the problem at hand, analysts commonly use a dashpot, in parallel with the retaining wall spring, in their model. In the present analysis the radiation energy loss may be considered, in an approximate manner, by assigning a higher value of damping to mode (or modes) with predominant retaining wall deformation. Since a fixed value of damping has been used for all modes of vibration (including those with predominant wall deformation), the radiation energy loss has not been completely ignored in the solutions presented.

Parametric studies

The plots of maximum base shear $(F_{sb})_{max}$ for different values of m_b/m, ζ, and T_w/T_f are shown in Figure 8. The base shear increases with increase in base mass, but remains nearly unaffected by changes in the damping

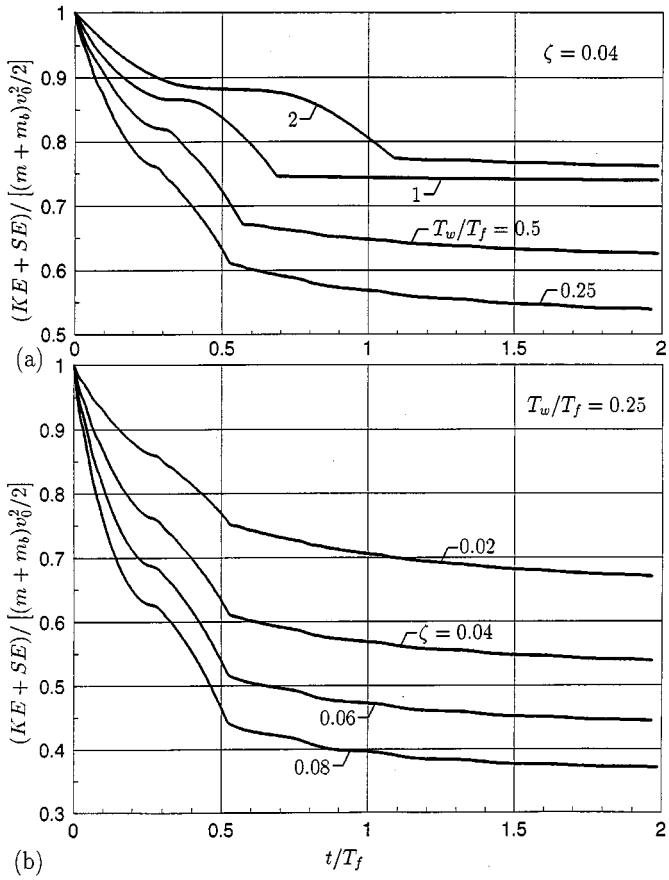

Figure 6. Timewise variation of total energy of the system for different values of (a) retaining wall stiffness; and (b) damping ratio ($m_b/m = 0{\cdot}2$)

ratio. The plots of maximum base displacement $(u_b)_{max}$ for different values of T_w/T_f and damping ratio ζ are shown in Figure 9(a). The base displacement increases with increase in wall flexibility and reduces slightly with increase in damping ratio. The effects of wall stiffness and damping ratio on the duration of impact τ are seen in Figure 9(b). Momentary loss of contact, for very stiff retaining walls, is not included in this plot. Note that the impact duration τ is equal to $T_f/2$ for a rigid wall, and $T_w/2$ for a rigid building. For other cases, τ is greater than both $T_f/2$ and $T_w/2$. The effect of a damping on τ is negligible.

Effect of assuming perfect isolation

Numerical results presented in this paper are based on the assumption that the isolation is perfect, i.e. the bearings have zero stiffness and damping. Since the bearing stiffness is small compared to retaining wall stiffness, the bearing stiffness can be neglected during impact. Since the deformation in the bearings is very small during impact, the damping in the bearings can also be neglected. Moreover, since the maximum shear force occurs during impact (Figure 4) and most of the system energy is lost during impact, the assumption of perfect isolation does not affect the values of maximum base shear and net energy loss in a significant way.

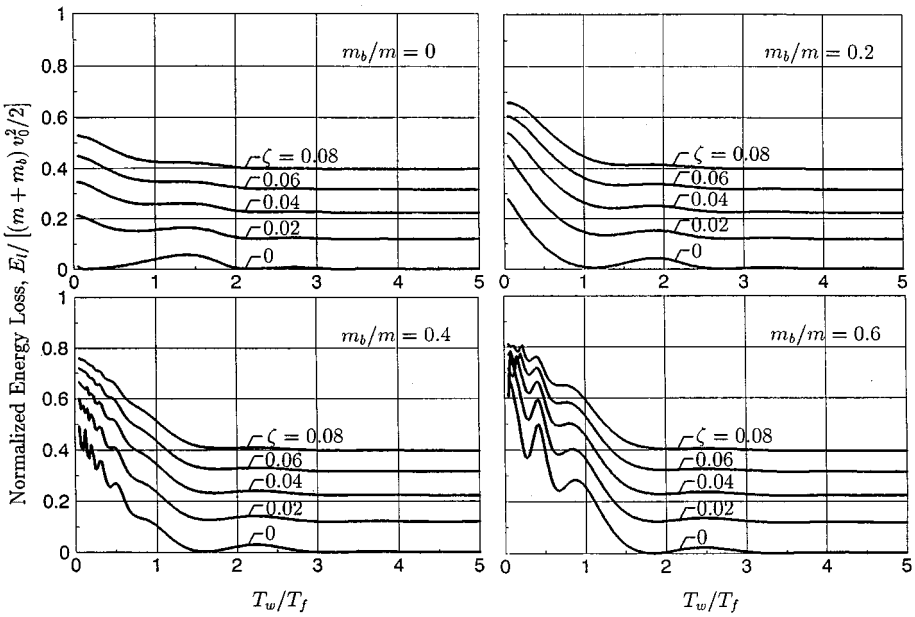

Figure 7. Total energy loss for different values of damping ratio, base mass and retaining wall stiffness

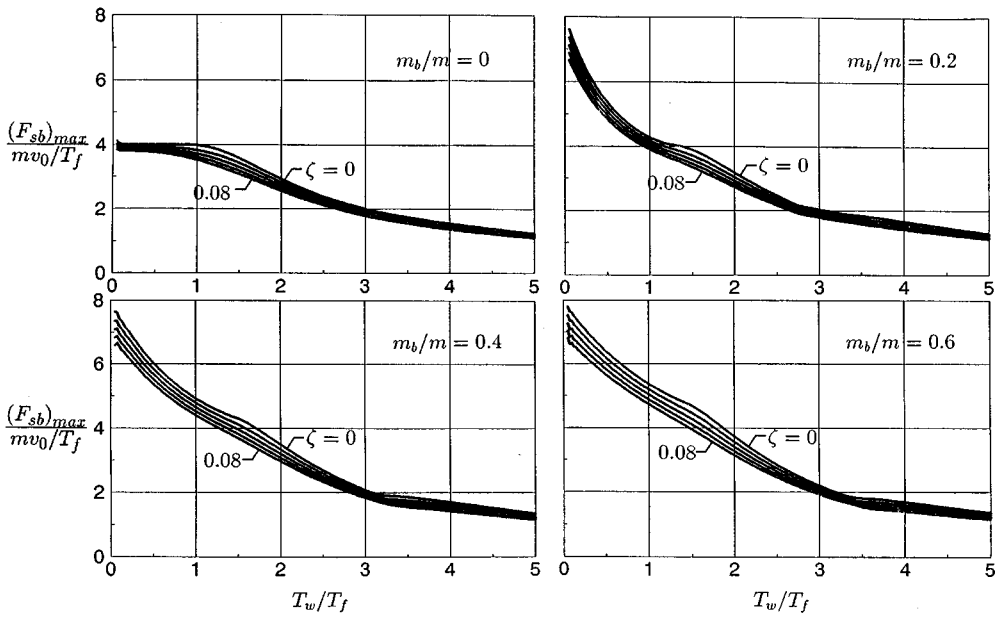

Figure 8. Maximum base shear for different values of damping ratio, base mass and retaining wall stiffness

CONCLUSIONS

Insight is gained into the dynamics of impact between the base of an isolated building and the surrounding retaining wall. The building is modelled by a uniform elastic shear beam and the retaining wall by an elastic

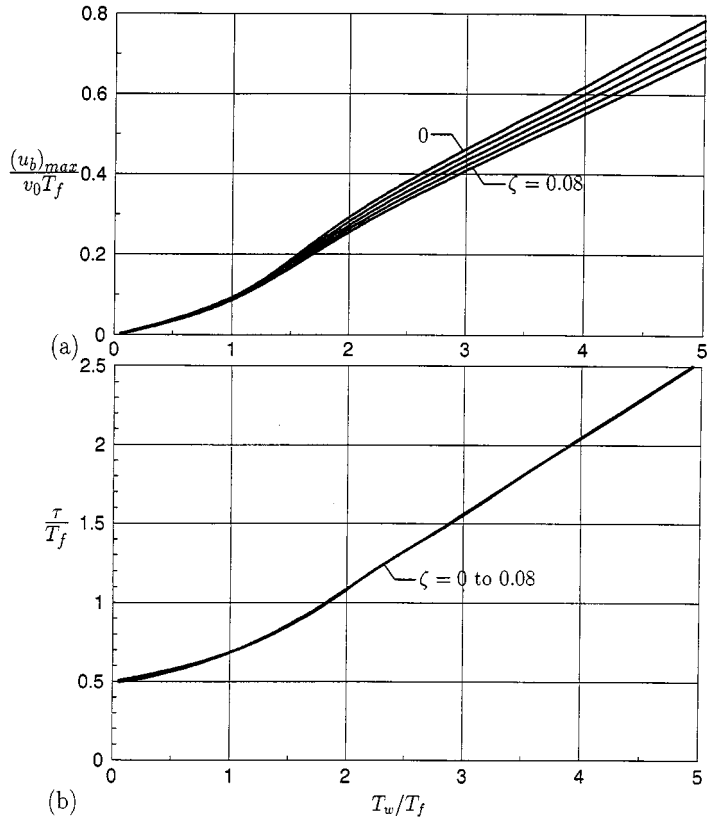

Figure 9. Effect of retaining wall stiffness and damping ratio on (a) maximum deformation of retaining wall and (b) duration of impact

spring. The analysis presented may be applied to any discrete system such as a building with finite number of modes. The following conclusions are based on the numerical results presented in this paper:

1. For an elastic system, the base shear generated by impact can be higher than the weight of the building. Its value is proportional to the impact velocity, and increases with increase in the stiffnesses of the building and the retaining wall. It also increases with increase in base mass, but remains nearly unaffected by changes in damping ratio.
2. In the presence of a base mass, the force in the retaining wall is higher than the base shear in the building. The effect of various parameters on the retaining wall force is similar to their effect on the base shear.
3. A significant amount of kinetic energy is lost as a result of impact. The loss of energy increases with increase in the base mass, system damping and retaining wall stiffness.
4. The duration of impact is equal to half the fundamental fixed-base period of the building for a rigid retaining wall, and half the period of the building–retaining wall system for a rigid building. For other cases, it is greater than both these values. Impact duration is not affected by damping ratio.

APPENDIX I

Notation

A	cross-sectional area of shear beam
c	shear wave velocity ($=\sqrt{G/\rho}$)
E_ℓ	net energy lost by impact
F_s	shear along the height of building
F_{sb}	shear at the base of building
$(F_{sb})_{max}$	maximum value of F_{sb}
F_w	force in retaining wall
g	acceleration due to gravity (981 cm/s^2)
H	height of shear beam
KE	kinetic energy
M	momentum of system
m	mass of the building excluding base mat ($=\rho AH$)
$\tilde{m}(\xi)$	distribution of mass along the height of the building [equation (6)]
m_b	mass of base mat
N	number of modes considered during impact
$\bar{N}$	number of modes considered after separation
SE	strain energy
T_f	fixed-base period of building [equation (1)]
T_w	period of building–retaining wall system assuming rigid building [equation (5)]
t	time measured from instant of impact
$\bar{t}$	time measured from separation ($=t-\tau$)
$U_{\bar{n}}$	displacement component of $\bar{n}$th mode of vibration after separation
u	horizontal displacement of a point on shear beam
u_b	horizontal displacement of base mat
$(u_b)_{max}$	maximum value of u_b
V_n	velocity component of nth mode of vibration during impact
$V_{\bar{n}}$	velocity component of $\bar{n}$th mode of vibration after separation
v	horizontal velocity of a point on shear beam
v_0	velocity of building and base mass at the instant of impact
v_b	velocity of base mat after separation
z	vertical distance measured from the top of base mat [Figure 1(b)]
ζ	modal damping ratio
ρ	mass density of shear beam
τ	duration of impact
ϕ_n	nth mode shape of system during impact
$\phi_{\bar{n}}$	$\bar{n}$th mode shape of system after separation
ω_n	frequency of nth mode of vibration during impact
$\omega_{n\mathrm{D}}$	damped natural frequency of nth mode of vibration during impact
$\omega_{\bar{n}}$	frequency of $\bar{n}$th mode of vibration after separation
$\omega_{\bar{n}\mathrm{D}}$	damped natural frequency of $\bar{n}$th mode of vibration after separation

APPENDIX II

Modal properties of system

Since the system is assumed classically damped, the system damping need not be considered in determining the mode shapes and undamped frequencies. The equation of equilibrium for the undamped shear beam in

Figure 1(b) is

$$\rho A\ddot{u}(\xi, t) - \frac{GA}{H^2}\frac{\partial^2 u(\xi, t)}{\partial \xi^2} = 0 \tag{40}$$

where the overdot denotes differentiation with respect to time. The boundary condition at the base of the shear beam ($\xi = 0$) is

$$m_b\ddot{u}_b(t) + k_w u_b(t) = -\rho AH\int_0^1 \ddot{u}(\xi, t)\,d\xi \tag{41}$$

and the boundary condition at the top of the shear beam ($\xi = 1$), obtained from no-shear condition, is

$$\frac{\partial u}{\partial \xi} = 0 \tag{42}$$

General solution of equation (40) may be expressed as

$$u(\xi, t) = \left\{A_n \cos\left(\frac{\omega_n H}{c}\xi\right) + B_n \sin\left(\frac{\omega_n H}{c}\xi\right)\right\}\sin(\omega_n t) \tag{43}$$

where $c = \sqrt{G/\rho}$ is the shear wave velocity, A_n and B_n are arbitrary constants and ω_n the nth natural frequency of the system. The base displacement, obtained from equation (43), is

$$u_b(t) = u(0, t) = A_n \sin(\omega_n t) \tag{44}$$

Substituting equations (43) and (44) into equation (41), we obtain

$$-m_b\omega_n^2 A_n + k_w A_n = \frac{m\omega_n c}{H}\left\{A_n \sin\left(\frac{\omega_n H}{c}\right) - B_n \cos\left(\frac{\omega_n H}{c}\right) + B_n\right\} \tag{45}$$

where $m = \rho AH$ is the mass of the shear beam. Substituting equation (43) into equation (42), we obtain

$$A_n \sin\left(\frac{\omega_n H}{c}\right) = B_n \cos\left(\frac{\omega_n H}{c}\right) \tag{46}$$

Using equation (46), equation (45) may be rewritten to give the following characteristic equation for determining the modal frequencies:

$$\tan\left(\frac{\omega_n T_f}{4}\right) = \left(\frac{T_f}{T_w}\right)^2\left(1 + \frac{m_b}{m}\right)\frac{\pi^2}{\omega_n T_f} - \frac{m_b}{m}\left(\frac{\omega_n T_f}{4}\right) \tag{47}$$

where $T_f = 4H/c$, and $T_w = 2\pi\sqrt{(m + m_b)/k_w}$. Using equation (46), equation (43) may be written as

$$u(\xi, t) = \frac{A_n \sin(\omega_n t)}{\cos(\omega_n H/c)}\left\{\cos\left(\frac{\omega_n H}{c}\right)\cos\left(\frac{\omega_n H}{c}\xi\right) + \sin\left(\frac{\omega_n H}{c}\right)\sin\left(\frac{\omega_n H}{c}\xi\right)\right\} \tag{48}$$

The term in brackets in equation (48) is the nth mode shape,

$$\phi_n(\xi) = \cos\left(\frac{\omega_n T_f}{4}\right)\cos\left(\frac{\omega_n T_f}{4}\xi\right) + \sin\left(\frac{\omega_n T_f}{4}\right)\sin\left(\frac{\omega_n T_f}{4}\xi\right) \tag{49}$$

REFERENCES

1. J. F. Hall, T. H. Heaton, M. W. Halling and D. J. Wald, 'Near-source ground motion and its effects on flexible buildings', *Earthquake spectra* EERI **11**(4), 569–605 (1995).
2. K. Kasai, W. D. Liu and V. Jeng, 'Effect of relative displacements between adjacent bridge segments', *Proc. SMIP92 seminar*, California Strong Motion Instrumentation Program, Sacramento, CA, 1992.

3. B. F. Maison and C. E. Ventura, 'Seismic analysis of base-isolated San Bernardino County building', *Earthquake spectra EERI* **8**(4), 605–633 (1992).
4. G. L. Fenves and R. Desroches, 'Evaluation of the response of I-10/215 Interchange bridge near San Bernardino in the 1992 Landers and Big Bear earthquakes', *Report CSMIP/95-02,* California Strong Motion Instrumentation Program, Sacramento, CA, 1995.
5. S. Nagarajaiah and S. Xiahong, 'Response of base isolated buildings during the 1994 Northridge earthquake', *SMIP95 seminar*, California Strong Motion Instrumentation Program, Sacramento, CA, 1995, pp. 41–55.
6. W. B. Cross and N. P. Jones, 'Seismic performance of joist-pocket connections. I: modeling', *J. struct. eng. ASCE* **119**(10), 2986–3007 (1993).
7. A. K. Chopra, *Dynamics of Structures: Theory and Applications to Earthquake Engineering*, Prentice-Hall, Englewood Cliffs, NJ, 1995.
8. K. F. Graff, *Wave Motion in Elastic Solids*, Clarendon Press, Oxford, London, 1975.
9. P. K. Malhotra, M. J. Huang and A. F. Shakal, 'Seismic interaction at separation joints of an instrumented concrete bridge', *Earthquake Engng. Struct. Dyn.* **24**, 1055–1067 (1995).

